
i-QER: AN INTELLIGENT APPROACH TOWARDS QUANTUM ERROR REDUCTION

Saikat Basu^{1,3*}, Amit Saha^{1,3}, Amlan Chakrabarti¹, Susmita Sur-Kolay²

¹A. K. Choudhury School of Information Technology, University of Calcutta

²Advanced Computing & Microelectronics Unit, Indian Statistical Institute

³Atos, Pune, India

*saikat.basu.000@gmail.com

ABSTRACT

Quantum computing has become a promising computing approach because of its capability to solve certain problems, exponentially faster than classical computers. An n -qubit quantum system is capable of providing 2^n computational space to a quantum algorithm. However, quantum computers are prone to errors. Quantum circuits that can reliably run on today's Noisy Intermediate-Scale Quantum (NISQ) devices are not only limited by their qubit counts but also by their noisy gate operations. In this paper, we have introduced *i*-QER, a scalable machine learning based approach to evaluate errors in a quantum circuit and help to reduce these without using any additional quantum resources. The *i*-QER predicts possible errors in a given quantum circuit using supervised learning models. If the predicted error is above a pre-specified threshold, it cuts the large quantum circuit into two smaller sub-circuits using an error influenced fragmentation strategy for the first time to the best of our knowledge. The proposed fragmentation process is iterated until the predicted error reaches below the threshold for each sub-circuit. The sub-circuits are then executed on a quantum device. Classical reconstruction of the outputs obtained from the sub-circuits can generate the output of the complete circuit. Thus, *i*-QER also provides a classical control over a scalable hybrid computing approach that is a combination of quantum and classical computers. The *i*-QER tool is available at <https://github.com/SaikatBasu90/i-QER>.

Keywords Quantum Error Reduction · Supervised Learning · Support Vector Regression · Quantum Circuit Fragmentation

1 Introduction

With the progress of quantum computing in the last two decades, modern researchers have exhibited a wondrous enthusiasm for realising quantum algorithms [1, 2, 3] to attain asymptotic improvement. Physical quantum computers employing various technologies, such as continuous spin systems [4], superconducting transmon technology [5], nuclear magnetic resonance [6, 7], photonic systems [8], ion trap [9], topological quantum systems [10], have reached new heights recently. It has become a blazing domain among the researchers to implement quantum algorithms [4] on the physical quantum devices. Every quantum algorithm can be realized in the form of a quantum circuit through qubits and quantum gates. Albeit the colossal promises of quantum algorithms, the present quantum computers are more error-prone, which limits the capability of solving a computation problem in quantum devices.

Quantum error correcting codes (QECCs) [11, 12, 13, 14, 15, 16, 17, 18, 19] are used to eradicate errors that arise from noise, to provide an avenue toward fault-tolerant quantum computation. However, in practice, the implementation of quantum error correction imposes a huge burden in terms of the required number of qubits, which remains beyond the capabilities of present near-term devices. Due to the typical error rate of current near-term devices, various error reduction techniques have emerged; one of them is quantum error mitigation (QEM) [20, 21]. QEM does not use any extra quantum resources, rather it aims to slightly enhance the accuracy of estimating the outcome in a given quantum

computational problem through several techniques such as extrapolation, probabilistic error cancellation, quantum subspace expansion, symmetry verification, machine learning etc. [20]. As per the state-of-the-art work, QEM is restricted to quantum circuits having a very limited number of qubits and limited depth due to the enormous overhead of classical computational time complexity.

In order to overcome the engineering challenges of QEM, fragmentation of quantum circuits can be a good approach because it breaks up quantum circuits into smaller sub-circuits or partitions, with fewer qubits and shallower depth. Thus the sub-circuits have to deal with short coherence times of noisy intermediate-scale quantum processor. Each sub-circuit faces a lower effect of noise when executed in a NISQ device. Primarily, fragmentation of a quantum circuit is used to simulate a larger quantum system on a small quantum computer [22, 23]. In [24, 25], the authors have proposed fragmenting a quantum circuit in such a way that the exponential post processing cost can be optimized. Further, in [26], the authors explored for the first time how such fragmentation affects the various quantum noise models. Later in [27], it was explored that circuit cutting helps to mitigate the effects of noise as portrayed in [26].

Our motivation: With this background, it is evident that fragmentation of a quantum circuit into smaller sub-circuits can reduce the effect of noise when executed in a NISQ device. Nonetheless, fragmentation increases post-processing cost, and thereby overall computational cost also escalates. In this paper, error reduction of a given circuit is carried out by predicting error in a quantum circuit, keeping into account that the fragmentation of a given quantum circuit is minimized. However, predicting error in a quantum circuit is a non-trivial problem. In this article, a machine learning based approach has been adopted for better accuracy in predicting the error in a quantum circuit by training the system considering the features of a quantum circuit. Our main contributions are as follows:

- a supervised machine learning based prediction technique to evaluate errors in a given quantum circuit;
- an error influenced fragmentation strategy called **Error Influenced Binary Quantum Circuit Fragmentation** based on the proposed prediction system has been introduced, to reduce the error of a quantum circuit; and
- an automated machine learning based tool *i*-QER i.e., **An Intelligent Approach towards Quantum Error Reduction** that helps to reduce the error of a quantum circuit that can be further incorporated for any existing quantum hardware. This tool also provides a classical control over hybrid quantum-classical computing.

The structure of this paper is as follows. Section 2 briefly presents the preliminary concepts of quantum circuits, quantum hardware, quantum circuit fragmentation and supervised machine learning models. Section 3 proposes the automated machine learning based approach *i*-QER. Section 4 briefly discusses about the experimental results of the proposed methodology. Section 5 captures our conclusions.

2 Background

2.1 Quantum Circuit

A quantum circuit is the schematic representation of any quantum algorithm or quantum program. Each line in the quantum circuit is expressed as a qubit and the operations, i.e., quantum gates are illustrated by different blocks on the line [28]. In Table 1, we summarize the commonly used logical quantum gates.

2.2 Quantum Hardware

Currently, the most popular quantum technologies for implementing the quantum gates are superconducting quantum devices, quantum dots, ion traps, neutral atoms. For mapping the synthesized quantum logic circuit to an existing noisy quantum hardware or NISQ (Noisy Inter-mediate Scale quantum) device [4], the logical quantum gates described in Table 1, must be realized by technology-specific gates to be hardware compatible for implementation. Each one of the devices based on the above mentioned technologies has a specifically dedicated qubit topology. For example, the arrangement for the 15-qubit IBM Melbourne quantum hardware [29] is shown in Figure 1. All the experiments of this paper are carried out on this machine.

Along with the constraint on the number of qubits, NISQ devices are “noisy”. Thus, estimation of the simulated result of a quantum state is erroneous. This error has to be reduced as much as possible, to get a proper estimation of the simulated result of a quantum state closer to its expected outcome.

Table 1: Matrix Representation of Quantum Gates

Operator	Quantum Gates	Matrix Representation
Hadamard		$\begin{pmatrix} \frac{1}{\sqrt{2}} & \frac{1}{\sqrt{2}} \\ \frac{1}{\sqrt{2}} & -\frac{1}{\sqrt{2}} \end{pmatrix}$
Pauli-X		$\begin{pmatrix} 0 & 1 \\ 1 & 0 \end{pmatrix}$
Pauli-Y		$\begin{pmatrix} 0 & -i \\ i & 0 \end{pmatrix}$
Pauli-Z		$\begin{pmatrix} 1 & 0 \\ 0 & -1 \end{pmatrix}$
T		$\begin{pmatrix} 1 & 0 \\ 0 & e^{i\pi/4} \end{pmatrix}$
S		$\begin{pmatrix} 1 & 0 \\ 0 & i \end{pmatrix}$
CNOT		$\begin{pmatrix} 1 & 0 & 0 & 0 \\ 0 & 1 & 0 & 0 \\ 0 & 0 & 0 & 1 \\ 0 & 0 & 1 & 0 \end{pmatrix}$
TOFFOLI		$\begin{pmatrix} 1 & 0 & 0 & 0 & 0 & 0 & 0 & 0 \\ 0 & 1 & 0 & 0 & 0 & 0 & 0 & 0 \\ 0 & 0 & 1 & 0 & 0 & 0 & 0 & 0 \\ 0 & 0 & 0 & 1 & 0 & 0 & 0 & 0 \\ 0 & 0 & 0 & 0 & 1 & 0 & 0 & 0 \\ 0 & 0 & 0 & 0 & 0 & 1 & 0 & 0 \\ 0 & 0 & 0 & 0 & 0 & 0 & 0 & 1 \\ 0 & 0 & 0 & 0 & 0 & 0 & 1 & 0 \end{pmatrix}$

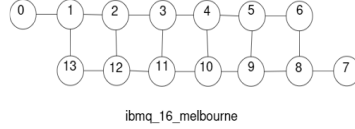


Figure 1: Qubit Topology [29]

2.3 Quantum Circuit Fragmentation

Fragmentation of a quantum circuit can be defined as a method for simulating large circuits by partitioning them into multiple weakly interacting partitions of smaller circuits. But in this paper, our main aim is to reduce the circuit error through fragmentation of a quantum circuit.

Four well-defined phases of the circuit fragmentation method are shown in Figure 2 [23]. Let us consider an example 4-qubit circuit C with three two-qubit gates as shown in Figure 2(a). All the input qubits are initialized with $|0\rangle$ and all the output qubits are measured in the same computational basis. Now, C can be described by a tensor network (G, A) consisting of a directed graph $G(E, V)$ and a collection of tensors $A = \{A(v) : v \in V\}$. In Figure 2(b), the corresponding tensor network of C is shown. As per conventional representation of a tensor network, the vertices V can be represented by individual gates (denoted by \square), input qubits (denoted by $\langle \rangle$), and measurement operators (denoted by \triangleright) as shown in Figure 2(b), considering that the flow of qubits is encoded by the directed edges E . For each $v \in V$, $A(v)$ is a tensor that encodes the matrix entries of the corresponding gate, state, or measurement operator, and the value $T(G, A)$ of the tensor network (G, A) occurs as the expected output of the corresponding circuit C . As shown in Figure 2(b), the two parts of a partition $\{S_1, S_2\}$ are indicated by a dashed line. Considering that only one qubit, i.e., the third qubit is sent from S_1 to S_2 as indicated by the red arrow, the value of K is 1, where K can be defined as the number of edges between the two partitions of G . Due to two outgoing edges from S_1 to measurement operators and one from S_1 to S_2 , the value of $d(S_1)$ is 3, where d can be defined as the number of qubits sufficient for simulating each partition. Similarly, the value of d for the partition of S_2 is 2 and therefore we can conclude that d is 3, by considering $\max(d(S_1), d(S_2))$. On that account, the example circuit C can be designated as (1, 3)-partitioned, as the values of K and d are 1 and 3 respectively. To simulate the two partitions on a 3-qubit quantum hardware, a

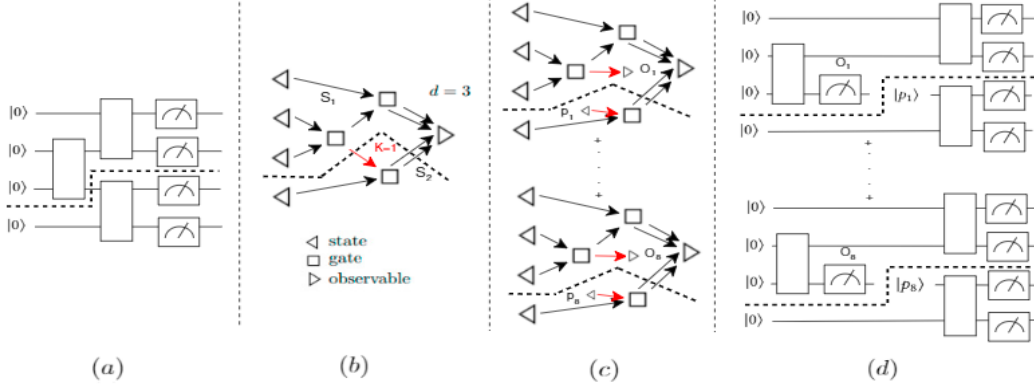


Figure 2: Four phases of quantum circuit fragmentation method as described in [23]: (a) an example quantum circuit; (b) its tensor network; (c) a collection of tensor networks obtained by cutting an edge; and (d) fragmented smaller quantum circuits for the example circuit.

well-defined edge-cutting procedure to realize the tensor networks as described in 2(b) is shown in Figure 2(c). After cutting an edge $e \in E$, the tensor $T(G(E, V), A)$ for the tensor network $(G(E, V), A)$ of the example circuit C can be mathematically represented as,

$$T(G, A) = \sum_{i=1}^8 c_i T(G', A_i), \quad (1)$$

where G' differs from G by removing e and adding one \triangleleft and one \triangleright vertex, each $c_i \in \{-\frac{1}{2}, \frac{1}{2}\}$, and each (G', A_i) corresponds to a valid quantum circuit. This can be further expressed in terms of intermediate measurement operator O_i and states p_i , where $1 \leq i \leq 8$. Thus, the tensor network is partitioned into two sub-circuits, which does not eventually affect the value of the overall tensor network. Each partition must have outgoing edges to the measurement operator and can hence be simulated by a 3-qubit quantum computer followed by classical processing of the measurement outcomes, as shown in Figure 2(d).

Here, the individual simulation results are combined by a simple sampling procedure according to Equation 1 where each Pauli matrix $\{I, X, Y, Z\}$ is expanded in its eigenbasis as denoted by O_i and their eigenprojectors p_i . Thus mathematically, \mathbf{A} , an arbitrary 2×2 matrix, can be realized as

$$\mathbf{A} = \frac{Tr(\mathbf{A}I)I + Tr(\mathbf{A}X)X + Tr(\mathbf{A}Y)Y + Tr(\mathbf{A}Z)Z}{2}. \quad (2)$$

To execute on quantum computers, Pauli matrices are further needed to be realised into their eigenbasis as follows

$$\mathbf{A} = \frac{A_1 + A_2 + A_3 + A_4}{2} \quad (3)$$

where

$$\begin{aligned} A_1 &= [Tr(\mathbf{A}I) + Tr(\mathbf{A}Z)] |0\rangle \langle 0| \\ A_2 &= [Tr(\mathbf{A}I) - Tr(\mathbf{A}Z)] |1\rangle \langle 1| \\ A_3 &= Tr(\mathbf{A}X) [2|+\rangle \langle +| - |0\rangle \langle 0| - |1\rangle \langle 1|] \\ A_4 &= Tr(\mathbf{A}Y) [2|+i\rangle \langle +i| - |0\rangle \langle 0| - |1\rangle \langle 1|] \end{aligned}$$

Each trace operator corresponds physically to measure the qubit in one of the Pauli bases $O_i \in \{I, X, Y, Z\}$ and each of the density matrices corresponds physically to initialize the qubit in one of the eigenstates $p_i \in \{|0\rangle, |1\rangle, |+\rangle, |+i\rangle\}$.

Later in [27], maximum-likelihood fragment tomography (MLFT) was introduced as an improved circuit cutting technique, with a limited number of qubits, to run partitioned quantum sub-circuits on quantum hardware. MLFT further finds the most likely probability distribution for the output of a quantum circuit, with the measurement data obtained from the circuit's fragments, along with minimizing the classical computing overhead of circuit cutting methods. Hence, they showed that circuit cutting as a standard tool can be used for running partitioned sub-circuits on quantum devices by estimating the outcome of a partitioned circuit with higher fidelity as compared to the full circuit execution. In this work, we have used a supervised machine learning based error influenced fragmentation strategy to cut the circuit into two partitions, described in next section.

2.4 Supervised Machine Learning

Machine Learning is the development of computing systems capable of learning automatically, without following explicit instructions. It uses algorithms or statistical models to extract inferences from patterns in the data [30]. Supervised learning algorithm is one of the key approaches of machine learning, which builds a mathematical model from a labelled data-set. The labelled data is known as training data, and consists of a set of training examples. Each training example consists of multiple feature values and the corresponding output label. The supervised learning algorithms used in this paper are described next.

2.4.1 Linear Regression:

This is a linear approach to model the relationship between a scalar response and one or more explanatory variables. In most linear regression models, given a training set of (x_i, y_i) , $i = 1, \dots, N$, where $x_i \in \mathbb{R}^n$ and $y \in \{1, -1\}^N$, the objective is to minimize the sum of squared errors,

$$\text{minimize } \sum_{i=1}^N (y_i - w_i x_i)^2 \quad (4)$$

where w_i represents the coefficients, or the weights of linear regression model. Linear regression is a special case of polynomial regression, which is also used in this work. Polynomial regression converts the original independent variables (x) of training data into polynomial features of required degree (2, 3, \dots , n). Therefore, it helps to make use of linear regression to train the more complicated non-linear data-set and increase the accuracy of the model.

2.4.2 Lasso Regression (Least Absolute Shrinkage and Selection Operator):

This is a special type of linear regression that uses shrinkage [31] where data values are shrunk towards a central point, say the mean. The lasso procedure encourages simple sparse models. Given a data-set of (X^i, y_i) , $i = 1, \dots, N$, where $X^i = (x_{i1}, \dots, x_{ip})^T$ are the predictor variables and $y \in \{1, -1\}^N$ are the responses, then the objective is to estimate Lasso $(\hat{\alpha}, \hat{\beta})$,

$$\text{minimize } \sum_{i=1}^N (y_i - \alpha - \sum_j \beta_j x_j)^2 \quad (5)$$

$$\text{subject to } |\beta_j| \leq t \quad (6)$$

where $t \geq 0$ is a tuning parameter, $\hat{\beta} = \{\hat{\beta}_1, \dots, \hat{\beta}_p\}^T$, and α is the parameter which balances the amount of emphasis given to minimization object. While $\alpha = 0$, Lasso regression produces the same coefficients as a linear regression.

2.4.3 Support Vector Regression:

The goal of a support vector machine (SVM) [32] is to produce a model based on the training data, which predicts the target values of the test data given only the test data attributes. SVM can also be used as a regression method, i.e., support vector regression (SVR), employing the same principles as the SVM for classification, with only a few minor differences. First of all, as the output is a real number it becomes very difficult to predict the information in hand, which has infinite possibilities. A margin of tolerance (ξ) is set in approximation to the SVM. Although the main goal is always the same, i.e., to minimize error, here the hyperplane which maximizes the margin (W, b), keeping in mind that part of the error is tolerated, is to be found. Given a training set of (x_i, y_i) , $i = 1, \dots, N$ where $x_i \in \mathbb{R}^n$ and $y \in \{1, -1\}^N$, the SVR requires the solution to the following optimization problem:

$$\text{minimize } \frac{1}{2} W^T W + C \sum_{i=1}^N (\xi_i + \xi_i^*) \quad (7)$$

$$\text{subject to } y_i - W^T x_i - b \leq \xi_i + \xi_i^*, \quad (8)$$

$$-y_i + W^T x_i + b \leq \xi_i + \xi_i^*, \quad (9)$$

$$\xi_i, \xi_i^* \geq 0 \quad (10)$$

where $C > 0$ is the penalty parameter of the error term.

The SVM is trained using a non-linear support vector regressor. A kernel function has to be chosen to implement support vector regression. The kernel function takes the original non-linear problem and transforms it into a linear one

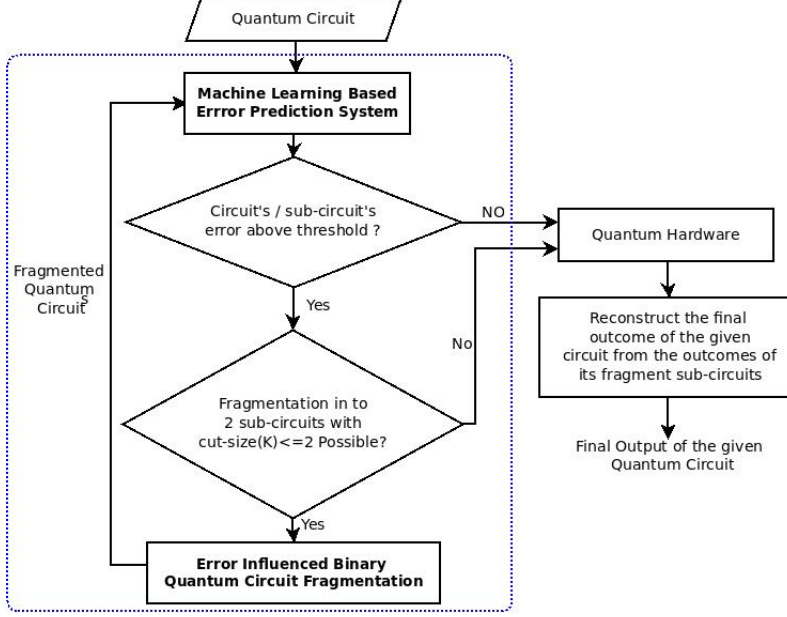


Figure 3: An overview of *i*-QER, an intelligent approach towards quantum error reduction using quantum circuit fragmentation. The blue dotted box contains the basic building blocks of the tool.

in the higher-dimensional space. One of the popular kernel functions is Radial basis function (RBF). The RBF kernel estimates the similarity between two points by non-linearly mapping them to the higher dimensional space[33]. Thus, it is capable of performing better than linear kernels in the presence of nonlinear attributes. Let us assume two points x_1 and x_2 , represented as a feature vector in a training data. Then, the kernel can be mathematically represented as

$$K(x_1, x_2) = \exp\left\{-\frac{\|x_1 - x_2\|^2}{2\sigma^2}\right\} \quad (11)$$

where $\|x_1 - x_2\|^2$ is the euclidean distance between x_1 and x_2 and σ is the variance. The equation can be rewritten as $K(x_1, x_2) = \exp(-\gamma\|x_1 - x_2\|^2)$, if we assume $\gamma = 1/2\sigma^2$.

2.4.4 Random Forest Regression:

A random forest is a predictor consisting of a collection of randomized base regression trees $\{r_n(\mathbf{x}, \Theta_m, \mathcal{D}_n), m \geq 1\}$, where $\Theta_1, \Theta_2, \dots$ are independent and identically distributed outputs of a randomizing variable Θ . These random trees are combined to form the aggregated regression estimate

$$\bar{r}_n(\mathbf{X}, \mathcal{D}_n) = \mathbb{E}_\Theta [r_n(\mathbf{X}, \Theta, \mathcal{D}_n)] \quad (12)$$

where \mathbb{E}_Θ denotes the expectation with respect to the random parameter, conditionally on \mathbf{X} and \mathcal{D}_n , a training data-set $\mathcal{D}_n = \{(\mathbf{X}_1, Y_1), \dots, (\mathbf{X}_n, Y_n)\}$ of independent and identically distributed random variables.

3 Proposed Methodology for *i*-QER

The details of our quantum error reduction tool *i*-QER is given next. The tool takes one quantum circuit as an input, and a supervised learning based error prediction system predicts the possible effects of noise on the quantum circuit when it is executed on a Noisy Intermediate-Scale Quantum (NISQ) device [4]. If the predicted effect of noise is beyond a threshold specified by the user, the circuit is fragmented [23] into two sub-circuits using a novel **Error Influenced Binary Quantum Circuit Fragmentation** strategy. The same process is repeated till the circuit is ready to be executed within an acceptable error rate. The sub-circuits are then executed on quantum hardware. The outcome of the full circuit is constructed from the outputs (probability distributions) of the sub-circuits. The output reconstruction of the full circuit is adopted from [23], which is already described in Section 2.3. Figure 3 provides a flow diagram of the tool incorporating the key components. Blocks written in bold are the main contributions of this paper and are described below.

3.1 Machine Learning Based Error Prediction System

3.1.1 Shots Finalisation

The prediction system learns from the previous performance of a particular quantum hardware and then performs its prediction accordingly. Any NISQ device executes a quantum circuit multiple times (shots). After each shot, all the qubits are measured and a classical output is recorded. After all the shots, a probability distribution over the observable states is returned. For a different number of shots, the output probability distribution has to be different. Hence, to construct accurate training data, it has to be generated with a fixed number of shots for all the benchmark circuits.

Quantum benchmark circuits [34] are executed with several possible shots and their corresponding errors are recorded. Based on these executed data, a polynomial curve of best fit is drawn using a polynomial regression model. An efficient shot with minimum error, is chosen using that curve. We are going to construct the training data-set based on that particular shot.

3.1.2 Training Data-set Construction

For any prediction model, a good training data on which the model can learn is mandated. The data-set has to contain the information about errors that occurred due to the noisy quantum computation. It must have all the major features of a quantum circuit and their corresponding errors that occurred while executing them on a NISQ device.

The impact of noise on a quantum circuit depends on a few major features, namely the number of different quantum gate operations, the number of qubits and the depth of the circuit. Hence, we need to extract the feature set for the training data based on these key components. The ideal measurement probabilities at a specific shot are compared with the actual measurement probabilities obtained under realistic noisy quantum hardware to obtain the dependent variable of the training data. We can describe probability vectors P_I^s and P_N^s to denote the ideal measurement probability and the actual noisy quantum hardware measurement probability respectively at a specific shot s . The error vector can be defined as $E^s = P_N^s - P_I^s$.

Table 2: Independent features of the constructed data-set for a given circuit

Circuit	# Gates of each of these 17 types	# Qubits	Depth
$H CNOT X Y Z R_X R_Y R_Z CZ CP/CU1 T Toffoli SWAP T^\dagger S S^\dagger U3$		Qubits	Depth

The features of the data-set used is specified in Table2. The complete data-set can be found at <https://github.com/SaikatBasu90/i-QER/dataset>

3.1.3 Machine Learning Model

Accurate prediction of error in a quantum circuit is a difficult task due to the dynamic nature of quantum circuits and their interactions with the environment. As the feature set of the constructed training data-set and the input training data is small in size, we have applied different supervised learning methodologies such as linear regression, lasso regression, random forest, support vector regression to predict the effects of noise in a quantum circuit for a particular NISQ device, instead of deep neural networks.

The experimental results appearing in Section 4 below established that the support vector regression with Radial Basis Kernel is the one which captures the effects of noise on quantum hardware better than the rest of the models. Therefore, we focus on support vector regression for further computation.

The best values of penalty parameter C and γ are not known a priori, when we need to fit a given problem to a SVM model with RBF kernel. There are no generalized rules to determine these parameters. So, we have used a two stage grid-search method [33] on C and γ with cross-validation on the data-set. A fine search is performed after a coarse search to find an optimal value

3.2 Error Influenced Binary Quantum Circuit Fragmentation

Once the error in a quantum circuit is predicted to be higher than a threshold, it is fragmented into more than one partition or sub-circuit. It helps in reducing the errors in each of the sub-circuits. A quantum circuit represented by a tensor network (G, A) consisting of a directed graph $G = (V, E)$ having n edges and a collection of tensors $A = \{A(v) : v \in V\}$ as described in Section 2.3, has a $\mathcal{O}(n!)$ combinatorial search space for all possible combinations of cut locations. But if the circuit is cut into two sub-circuits, the cut location search space reduces to $\mathcal{O}(n)$.

Our objective is to reduce the error while minimizing the number of fragments. We want to cut the circuit into two circuit partitions with low correlation or entanglement between them. Cutting the circuit into two sub-circuits, makes it a special case where K , the number of qubits communicating between the sub-circuits () become the upper bound of entanglement or correlation between them. To ensure low entanglement we choose to allow K to be at most 2. This constraint also ensures lower classical post processing cost. Therefore, we cut the quantum circuit if and only if there is an edge or cut location with $K \leq 2$. To reduce the error, our approach towards fragmentation is to cut the circuit in such a way that each of the partitions share approximately equal errors. We have applied a binary search based on error prediction of quantum circuits, **Error Influenced Binary Cut Selector algorithm** to select a cut location.

Algorithm 1: Error Influenced Binary Cut selector

Input: K , cut size i.e., the number of qubits communicating between the sub-circuits; n , the number of such cut locations where cut size $K \leq 2$; partitions
Output: Selected Cut Location Index
 // Consider all the edges or cut locations where $K \leq 2$ as an input.
 // Calculate errors for each cut location
for $i=1$ to n **do**
 // Predict Errors in each of the partitions using ML Based Prediction system
 E_{P_1} = machine learning based error prediction ($Partition_{i1}$);
 E_{P_2} = machine learning based error prediction ($Partition_{i2}$);
 // Calculate absolute difference of error between the partitions for each cut
 $Distance_i = |E_{P_1} - E_{P_2}|$;
end
 // Find the minimum $Distance_i$, for $1 \leq i \leq n$
 $Index =$ index of cut location at $\min(Distance_i)$;
return $Index$

Algorithm 1 considers each of the edges along with their corresponding partitions and predicts their corresponding errors. Let us assume a cut location index i , having two partitions $Partition_{i1}$ and $Partition_{i2}$. Algorithm 1 invokes the machine learning based prediction system to predict the errors in each of the two partitions. Further, it estimates how close these two partitions are with respect to the errors, i.e., $Distance_i$ is the absolute difference in error for the partitions $i1$ and $i2$. The algorithm returns the index of the cut whose $Distance$ value is minimum.

4 Experimental Results

In this section, we describe the experimental data at each step. While the tool can be applied on any quantum hardware, we have considered 15-qubit IBM Melbourne device for our experiments. The first step is to identify the iteration or shot for which the entire experiment will be performed. For that purpose, we have performed a search on the shots to identify the best performing shot with respect to the errors in a quantum circuit. We have applied polynomial linear regression on the data collected from the benchmark circuits, when executed on 15-qubit IBM Melbourne device.

Figure 4 shows the error behavior of quantum circuits with respect to shots or iterations. The X axis of the plot gives the shot number in log-scale, i.e., the number of shots is 2^X , and the Y axis denotes the mean of the absolute error in the circuits run for the corresponding number of shots. We have drawn a polynomial line of best fit using linear regression to identify a better performing shot. The experimental results show that circuits have better performance with respect to the errors for the shot number $2^7 = 128$ marked as a red point on the plot.

Performance of machine learning models: We have run 75 different benchmark circuits from [34, 35] in the 15-qubit IBM Melbourne device with the specified shot, to collect the training data. We have compared their output probability distribution with their corresponding ideal simulation output. Then we have computed the corresponding error as the mean absolute error, $E_{mean} = \frac{1}{N} \sum_{i=1}^N |y_s - y_q|$ and root mean square error $E_{rmse} = \sqrt{\frac{1}{N} \sum_{i=1}^N (y_s - y_q)^2}$. Here y_s and y_q are the output of the ideal simulator and noisy quantum hardware respectively and N is the number of output marked states. Here we have considered output to be the probability (in percentage) of marked states.

To perform testing on the machine learning based prediction model we have split the constructed data-set into two parts with 80% as training data and the rest 20% as test data.

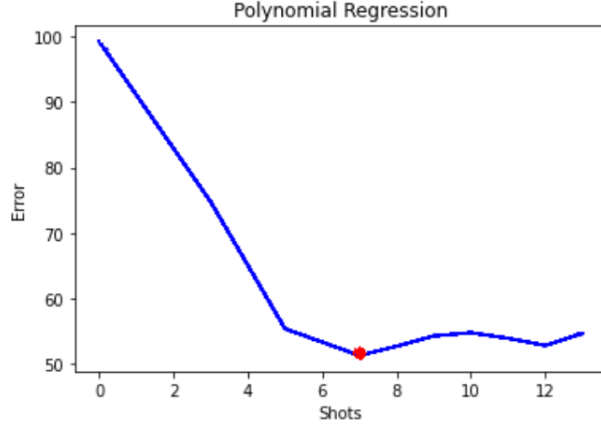


Figure 4: Performance of benchmark circuits executed on 15 qubit IBM Melbourne hardware with different shots ($\log_2(\text{shots})$) plotted in the X-axis and their corresponding mean absolute error (%) plotted in the Y-axis

As mentioned in the Section 3.1, for choosing C and γ while performing SVR, we have applied the grid search. At first a coarse search with $C=1, 1000, 2000, \dots, 50000$; and $\gamma=1, 2, 3$ is performed to identify the near to optimal values. After that, a fine search with $C=10, 20, 30, \dots, 1000$ and $\gamma=0.001, 0.01, 0.1, 1$ is done to identify the optimum values.

The performance of the various machine learning models trained on thus constructed data-set is assessed with respect to the output generated by the models, when they are verified on test data. Root Mean Square Error (RMSE) is taken as a performance measure in this work. The coefficient of determination known as the R^2 score, on test data has also been evaluated for all the models. R^2 is defined as follows:

$$R^2 = 1 - \frac{SS_R}{SS_T} \quad (13)$$

where SS_R is the sum of squares of the residuals or the prediction error and SS_T is the total sum of squares. Let us consider an example of the first circuit (Shor's algorithm) in Table 4, where the actual error of the circuit is 64.343% and our prediction system has predicted it to be 59.210%. Here, $SS_R = (64.343 - 59.210)^2 = 5.133^2 = 26.347$ and $SS_T = 64.343^2 = 4140.021$. Hence the $R^2 = 1 - \frac{26.347}{4140.021} = 0.993$. The best possible R^2 score is 1 and it may also take negative value when the model is arbitrarily worse.

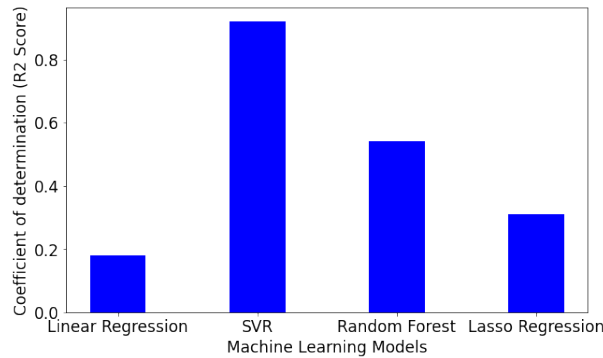


Figure 5: Comparison of R^2 score for the machine learning models on our test data: Linear Regression, Lasso Regression, Random Forest and Support Vector Regression (SVR)

We have trained four supervised learning models: linear regression, lasso regression, support vector regression and random forest. The performance of these models on test data with respect to predicted R^2 scores is given in the Figure 5 with SVR out-performing the other models.

A detailed analysis based on the performance of the machine learning models on benchmark test circuits is given in the Table 3 (best values written in bold). We have compared machine learning models with respect to root mean squared error(RMSE), mean squared error(MSE), mean error, R^2 and adjusted R^2 score and it can be observed that support

Table 3: Performance of machine learning models on test data

ML Models	RMSE	MSE	Mean Error	R^2 Score	Adjusted R^2
Linear Regression	31.61	999.51	26.40	0.18	-0.02
Lasso Regression	29.03	842.93	24.95	0.31	-0.019
Random Forest	23.67	560.44	18.19	0.54	0.32
Support Vector Regression	10.079	101.59	8.42	0.92	0.88

vector regression (SVR) model performs better than the other three supervised learning models. Hence, we have used the SVR model in our proposed prediction system *i*-QER.

Quantum circuit for validating the proposed tool *i*-QER: We run our tool on a quantum circuit before executing it in the real quantum hardware, say 15-qubit IBM Melbourne device. Further, we also verify the results of *i*-QER with that from the actual quantum hardware.

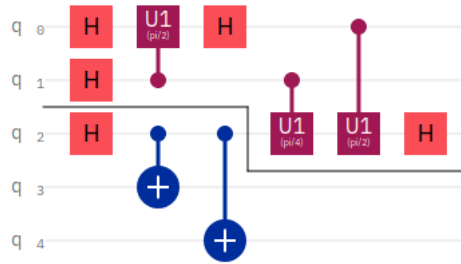


Figure 6: Implementation of error influenced binary circuit fragmentation on 5 qubit Shor’s algorithm

Figure 6 is a circuit for 5-qubit Shor’s algorithm. We execute the circuit in the proposed tool. First, let us consider the pre-specified threshold value for absolute error to be 50%. Our prediction model has predicted the absolute error of the circuit to be 59.210%. As it is higher than the threshold value, the circuit has been fragmented. We have applied **Error Influenced Binary Cut Selector** algorithm to cross check all possible cuts with $K \leq 2$. The algorithm selected the cut with an absolute error difference of 15.94% between the partitions, on the qubit q_2 . We cut the circuit as shown in Figure 6 into two circuit partitions. We apply the prediction model to the circuit partitions to predict their errors. As per the prediction system, sub-circuit 1 has absolute error of 10.05% and sub-circuit 2 has an absolute error of 25.99%. The predicted errors are below the pre-specified threshold, so these two can be directly executed on the actual hardware, where these are found to have 14.511% and 39.06% absolute error respectively. After reconstruction of the full evaluation of the circuit from the outputs of its sub-circuit partitions, we get a mean absolute error of 47.90. So the absolute error in the circuit has been reduced by 26.129%.

Table 4: Quantum circuits executed in *i*-QER and verified with corresponding actual hardware results

Quantum Circuit	Actual Error (%)		Predicted Error (%)		Error After Reconstruction (%)	Error Reduction (%)
	Full circuit	Fragments	Full circuit	Fragments		
Shor’s algorithm	64.843	14.511 , 39.06	59.210	10.05 , 25.99	47.90	26.129
BVS algorithm	96.09	22.656 , 49.22	86.48	22.077 , 42.656	60.72	36.809
$Amod5 - v0_20$	82.81	36.75 , 46.562	70.867	32.750 , 41.727	66.20	20.057
Toffoli double	62.50	29.6875 , 13.4375	68.439	24.366 , 5.487	39.135	37.382

Similarly, we have executed benchmark circuits and the results of these experiments are shown in Table 4. On an average, the absolute error in those circuits has been reduced by 30.095%.

5 Conclusion

We developed a scalable classical machine learning based system *i*-QER to reduce errors in a quantum circuit. Supervised machine learning models are trained using the error behavior of the benchmark quantum circuits when executed in a quantum hardware, to predict the amount of errors in an unknown quantum circuit. Further, if the predicted error is higher than a threshold limit the circuit is fragmented. We have proposed a novel error-influenced fragmentation

strategy, **Error Influenced Binary Quantum Circuit Fragmentation** to ensure lower errors in the fragmented circuit partitions. We iterate the same procedure till the error gets reduced below the threshold. To estimate the final evaluation of the quantum circuit, we reconstruct the output probability distributions of the circuit partitions. The proposed system successfully reduced the error in quantum circuits when we conducted experiments on different quantum circuits. The tool *i*-QER not only reduces error but also provides a classical control over a hybrid quantum-classical computing environment. Even if the present NISQ devices scale to a larger size, this *i*-QER tool with its error efficient classically controlled hybrid computing approach can bring more accuracy towards realistic quantum computing applications. In future, we plan to implement our approach for other quantum hardware settings. The results are very promising to pave the way for further research using different machine learning or neural network models on more benchmark circuits.

Acknowledgments

There is no conflict of interest.

References

- [1] Michael A. Nielsen and Isaac L. Chuang. *Quantum Computation and Quantum Information: 10th Anniversary Edition*. Cambridge University Press, 2010.
- [2] Lov K. Grover. A fast quantum mechanical algorithm for database search. In *Proceedings of the Twenty-eighth Annual ACM Symposium on Theory of Computing*, STOC '96, pages 212–219, New York, NY, USA, 1996. ACM.
- [3] Peter W. Shor. Polynomial-time algorithms for prime factorization and discrete logarithms on a quantum computer. *SIAM Journal on Computing*, 26(5):1484–1509, Oct 1997.
- [4] John Preskill. Quantum Computing in the NISQ era and beyond. *Quantum*, 2:79, August 2018.
- [5] Jens Koch, Terri M. Yu, Jay Gambetta, Andrew A. Houck, David I. Schuster, Johannes Majer, Alexandre Blais, Michel H. Devoret, Steven M. Girvin, and Robert J. Schoelkopf. Charge-insensitive qubit design derived from the cooper pair box. *Phys. Rev. A*, 76:042319, Oct 2007.
- [6] Shruti Dogra, Arvind, and Kavita Dorai. Determining the parity of a permutation using an experimental nmr qutrit. *Physics Letters A*, 378(46):3452–3456, Oct 2014.
- [7] Zafer Gedik, Isabela A. Silva, Barış Çakmak, Göktuğ Karpat, E. L. G. Vidoto, Diogo O. Soares-Pinto, Eduardo R. deAzevedo, and Felipe F. Fanchini. Computational speed-up with a single qudit. *Scientific Reports*, 5(1), Oct 2015.
- [8] Sergei Slussarenko and Geoff J. Pryde. Photonic quantum information processing: A concise review. *Applied Physics Reviews*, 6(4):041303, Dec 2019.
- [9] Colin D. Bruzewicz, John Chiaverini, Robert McConnell, and Jeremy M. Sage. Trapped-ion quantum computing: Progress and challenges. *Applied Physics Reviews*, 6(2):021314, Jun 2019.
- [10] Shawn X. Cui and Zhenghan Wang. Universal quantum computation with metaplectic anyons. *Journal of Mathematical Physics*, 56(3):032202, Mar 2015.
- [11] Markus Grassl, Willi Geiselmann, and Thomas Beth. Quantum reed—solomon codes. In Marc Fossorier, Hideki Imai, Shu Lin, and Alain Poli, editors, *Applied Algebra, Algebraic Algorithms and Error-Correcting Codes*, pages 231–244, Berlin, Heidelberg, 1999. Springer Berlin Heidelberg.
- [12] Daniel Gottesman. Fault-tolerant quantum computation with higher-dimensional systems. In Colin P. Williams, editor, *Quantum Computing and Quantum Communications*, pages 302–313, Berlin, Heidelberg, 1999. Springer Berlin Heidelberg.
- [13] Chungheon Baek, Tomohiro Ostuka, Seigo Tarucha, and Byung-Soo Choi. Density matrix simulation of quantum error correction codes for near-term quantum devices. *Quantum Science and Technology*, 5(1):015002, dec 2019.
- [14] Michael N. Leuenberger and Daniel Loss. Quantum computing in molecular magnets. *Nature*, 410(6830):789–793, Apr 2001.
- [15] Peter W. Shor. Scheme for reducing decoherence in quantum computer memory. *Phys. Rev. A*, 52:R2493–R2496, Oct 1995.
- [16] Andrew M. Steane. Error correcting codes in quantum theory. *Phys. Rev. Lett.*, 77:793–797, Jul 1996.
- [17] James R Wootton. Benchmarking near-term devices with quantum error correction. *Quantum Science and Technology*, 5(4):044004, aug 2020.

- [18] Barbara M. Terhal. Quantum error correction for quantum memories. *Rev. Mod. Phys.*, 87:307–346, Apr 2015.
- [19] Raymond Laflamme, Cesar Miquel, Juan Pablo Paz, and Wojciech Hubert Zurek. Perfect quantum error correcting code. *Phys. Rev. Lett.*, 77:198–201, Jul 1996.
- [20] Hendrik Poulsen Nautrup, Nicolas Delfosse, Vedran Dunjko, Hans J. Briegel, and Nicolai Friis. Optimizing quantum error correction codes with reinforcement learning. *Quantum*, 3:215, Dec 2019.
- [21] Changjun Kim, Kyungdeock Daniel Park, and June-Koo Rhee. Quantum error mitigation with artificial neural network. *IEEE Access*, 8:188853–188860, 2020.
- [22] Sergey Bravyi, Graeme Smith, and John A. Smolin. Trading classical and quantum computational resources. *Physical Review X*, 6(2), Jun 2016.
- [23] Tianyi Peng, Aram W. Harrow, Maris Ozols, and Xiaodi Wu. Simulating large quantum circuits on a small quantum computer. *Phys. Rev. Lett.*, 125:150504, Oct 2020.
- [24] Wei Tang, Teague Tomesh, Martin Suchara, Jeffrey Larson, and Margaret Martonosi. Cutqc: Using small quantum computers for large quantum circuit evaluations. In *Proceedings of the 26th ACM International Conference on Architectural Support for Programming Languages and Operating Systems*, ASPLOS 2021, page 473–486, New York, NY, USA, 2021. Association for Computing Machinery.
- [25] Thomas Ayril, François-Marie Le Régent, Zain Saleem, Yuri Alexeev, and Martin Suchara. Quantum divide and compute: Hardware demonstrations and noisy simulations. In *2020 IEEE Computer Society Annual Symposium on VLSI (ISVLSI)*, pages 138–140, 2020.
- [26] Thomas Ayril, François-Marie Le Régent, Zain Saleem, Yuri Alexeev, and Martin Suchara. Quantum divide and compute: Exploring the effect of different noise sources, 2021.
- [27] Michael A. Perlin, Zain H. Saleem, Martin Suchara, and James C. Osborn. Quantum circuit cutting with maximum-likelihood tomography. *npj Quantum Information*, 7:1–8, 2021.
- [28] Adriano Barenco, Charles H. Bennett, Richard Cleve, David P. DiVincenzo, Norman Margolus, Peter W. Shor, Tycho Sleator, John A. Smolin, and Harald Weinfurter. Elementary gates for quantum computation. *Phys. Rev. A*, 52:3457–3467, Nov 1995.
- [29] IBM Quantum. Ibm q 16 melbourne backend specification. June 2021.
- [30] Ethem Alpaydin. *Introduction to Machine Learning*. The MIT Press, 2nd edition, 2010.
- [31] Robert Tibshirani. Regression shrinkage and selection via the lasso. *Journal of the royal statistical society series b-methodological*, 58:267–288, 1996.
- [32] Vladimir N. Vapnik. *The nature of statistical learning theory*. Springer-Verlag New York, Inc., 1995.
- [33] Chih-wei Hsu, Chih-chung Chang, and Chih-Jen Lin. A practical guide to support vector classification chih-wei hsu, chih-chung chang, and chih-jen lin. 11 2003.
- [34] Ang Li and Sriram Krishnamoorthy. Qasmbench: A low-level qasm benchmark suite for nisq evaluation and simulation, 2020.
- [35] Robert Wille, Daniel Große, Lisa Teuber, Gerhard W. Dueck, and Rolf Drechsler. Revlib: An online resource for reversible functions and reversible circuits. In *38th International Symposium on Multiple Valued Logic (ismvl 2008)*, pages 220–225, 2008.